



HAL
open science

Modeling the temperature effect on the specific growth rate of phytoplankton: a review

Ghjuvan Micaelu Grimaud, Francis Mairet, Antoine Sciandra, Olivier Bernard

► To cite this version:

Ghjuvan Micaelu Grimaud, Francis Mairet, Antoine Sciandra, Olivier Bernard. Modeling the temperature effect on the specific growth rate of phytoplankton: a review. *Reviews in Environmental Science and Bio/technology*, 2017, 10.1007/s11157-017-9443-0 . hal-01576871

HAL Id: hal-01576871

<https://inria.hal.science/hal-01576871>

Submitted on 24 Aug 2017

HAL is a multi-disciplinary open access archive for the deposit and dissemination of scientific research documents, whether they are published or not. The documents may come from teaching and research institutions in France or abroad, or from public or private research centers.

L'archive ouverte pluridisciplinaire **HAL**, est destinée au dépôt et à la diffusion de documents scientifiques de niveau recherche, publiés ou non, émanant des établissements d'enseignement et de recherche français ou étrangers, des laboratoires publics ou privés.

Modeling the temperature effect on the specific growth rate of phytoplankton: a review

Ghjuvan Micaelu Grimaud · Francis Mairet ·
Antoine Sciandra · Olivier Bernard

Received: date / Accepted: date

Abstract Phytoplankton are key components of ecosystems. Their growth is deeply influenced by temperature. In a context of global change, it is important to precisely estimate the impact of temperature on these organisms at different spatial and temporal scales. Here, we review the existing deterministic models used to represent the effect of temperature on microbial growth that can be applied to phytoplankton. We first describe and provide a brief mathematical analysis of the models used in constant conditions to reproduce the thermal growth curve. We present the mechanistic assumptions concerning the effect of temperature on the cell growth and mortality, and discuss their limits. The coupling effect of temperature and other environmental factors such as light are then shown. Finally, we introduce the models taking into account the acclimation needed to thrive with temperature variations. The need for new thermal models, coupled with experimental validation, is argued.

Keywords Temperature growth models, thermal growth curve, protein thermal stability, phytoplankton, microalgae, cyanobacteria

1 Introduction

1 Recent estimations predict a global temperature increase of 1°C to 5°C by the year 2100 (Rogelj
2 et al, 2012). In this context, the microbial communities, either terrestrial or aquatic, are expected
3 to be deeply impacted (Frey et al, 2013; Vezzulli et al, 2012; Thomas et al, 2012). Unicellular
4 organisms are ectotherms and cannot regulate their temperature. They are thus particularly sensi-
5 tive to temperature, which controls cellular metabolism by affecting enzymatic activity (Privalov,
6 1979; Kingsolver, 2009) and stability (Privalov, 1979; Danson et al, 1996; Eijsink et al, 2005).
7 Microorganisms play a key ecological role since they are involved in most of the biogeochemical
8 fluxes (Paul, 2014; Fuhrman et al, 2015). Especially, the autotrophic unicellular organisms (*i.e.*
9 phytoplankton) are the basis of trophic chains in the majority of ecological systems (Field et al,
10 1998). Modeling the effect of temperature on phytoplankton physiology and cellular metabolism is
11 thus crucial for better predicting ecosystems evolution in a changing environment.

12 In balanced growth conditions, the net growth rate of every microorganism as a function of
13 temperature is an asymmetric curve (see fig. 1) called the thermal growth curve or the thermal
14 reaction norm (Kingsolver, 2009). The cardinal temperatures corresponding to the boundaries of
15 thermal tolerance are defined as the minimal (T_{min}) and maximal (T_{max}) temperatures for growth.
16 The temperature for which growth is maximal is called the optimal temperature (T_{opt}). The growth
17 rate obtained at T_{opt} is the maximal growth rate μ_{opt} , whenever all the other factors affecting
18 growth are non-limiting. The thermal range on which a given species can thrive is the thermal

Ghjuvan Micaelu Grimaud · Francis Mairet · Olivier Bernard
BIOCORE-INRIA, BP93, 06902 Sophia-Antipolis Cedex, France. E-mail: grimaudg@msu.edu

Antoine Sciandra
UPMC Univ Paris 06, UMR 7093, LOV, Observatoire oceanologique, F-06234, CNRS, UMR 7093, LOV, Observatoire
oceanologique, F-06234, Villefranche/mer, France.

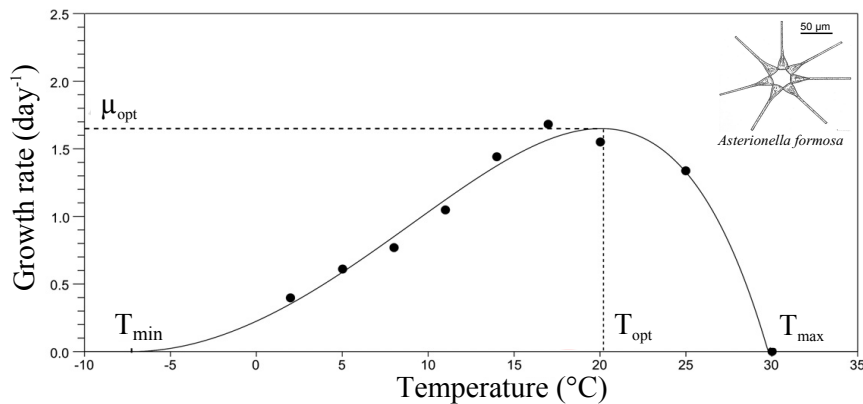


Fig. 1 Thermal growth curve of the microalgae species *Astrionella formosa* (redrawn from Bernard and Rémond (2012)).

19 niche width (*i.e.* $T_{max} - T_{min}$). The asymmetry of the growth curve results from differential effects
 20 on physiology at low (under T_{opt}) and high (above T_{opt}) temperatures. At low temperatures the
 21 rate of every enzymatic biochemical reactions are affected. At high temperatures, structure and
 22 stability of some cellular components, such as key enzymes or membrane compounds (mainly lipids
 23 or proteins) are denatured. The consequences on cell metabolism and integrity leads to an increase
 24 in mortality (Serra-Maia et al, 2016). These deleterious effects depend on the time spent at high
 25 temperature, while the ‘thermal dose’ represent the temperature damages (Holcomb et al, 1999).
 26 The combined effects on metabolism, cell regulation mechanisms and cell integrity give the thermal
 27 growth curve (Corkrey et al, 2014; Ghosh et al, 2016). While most of these underlying mechanisms
 28 have not been fully elucidated, several authors have proposed macroscopic models to represent this
 29 thermal growth curve. These simple models account for a minimum number of variables and do
 30 not provide a detailed mechanistic description of the involved biochemical underlying phenomena.

31 The aim of this study is to summarize the existing deterministic temperature growth models
 32 that can be used for phytoplankton, and to clarify the assumptions on the considered physiological
 33 processes. Firstly, models in non-limited and balanced growth conditions (*i.e.* when all the cell
 34 variables grow at the same constant rate over time) are described. The key hypotheses are explored
 35 through the review of growth models as well as the representation of the effect of temperature on
 36 cell mortality. Secondly, the coupling effect of temperature and other environmental factors such as
 37 light is addressed. Thirdly, a guideline is proposed to choose a model depending on the modelling
 38 purposes. Then, we present models taking into account temperature variations. The challenges to
 39 design a new generation of thermal models are finally discussed.

Model	Type	# Parameters	Validation (data sets)	Cardinal temperatures	Mortality
Empirical models					
Square-root	E	4	29, bacteria (Ratkowsky et al, 1983)	T_{min} and T_{max} are explicit T_{opt} is found by numerical optimization	No
CTMI	E	4	47, bacteria & yeast (Rosso et al, 1993)	Explicit	No
Blanchard	E	4	2, benthic phytoplankton (Blanchard et al, 1996)	T_{opt} and T_{max} are explicit T_{min} is not defined	No
Bernard&Rémond	E	4	15, phytoplankton (Bernard and Rémond, 2012)	Explicit	No
Eppley-Norberg	SE	4	5, phytoplankton (Norberg, 2004)	$T_{opt} = \frac{bz - 1 + \sqrt{(w/2)^2 b^2 + 1}}{b}$ $\text{abs}(T_{max} - T_{min}) = w$	No
Semi-empirical models					
Arrhenius equation	SE	2	-	Not defined	No
General mechanistic models					
Master reaction (for eq. 19)	M	4	1, normalized, bacteria (Johnson and Lewin, 1946) and then yeast (Van Uden, 1985)	$T_{opt} = \frac{\Delta H^\ddagger / R}{\ln\left(\frac{-\Delta H^\ddagger e^{\Delta S} - \Delta H e^{\Delta S}}{\Delta H}\right)}$ T_{min} and T_{max} are not defined	Yes (implicit)
Hinshelwood	M	4	No	$T_{opt} = \frac{E_1 - E_2}{R \ln\left(\frac{A_1 E_1}{A_2 E_2}\right)}$ $T_{max} = \frac{E_1}{R \ln\left(\frac{A_1}{A_2}\right)}$ $T_{min} = T_{opt} \left(\frac{-E_1/\gamma}{T_{opt} - E_2/\gamma}\right)$ with $\gamma = R \ln(A_2/A_1 e^{(E_2 - E_1)/E_1})$	Yes (explicit)
DEB theory	M	6	No	T_{min} and T_{max} are not defined T_{opt} is found numerically	Yes (implicit)
Protein-stability based models					
Modified Master reaction	M	4	230, normalized, all microorganisms (Corkrey et al, 2014)	$T_{opt} = \frac{\Delta C_p T_0 + \Delta H}{\Delta C_p + R}$ T_{min} and T_{max} are not defined	Yes (implicit)
Proteome based	M	2	12, normalized, bacteria (Dill et al, 2011)	T_{min} and T_{max} are not defined T_{opt} is found numerically	Yes (implicit)
Heat capacity based	M	4	12, soil processes (Schipper et al, 2014)	$T_{min}, T_{opt}, T_{max}$ are found numerically	No

Table 1 Synthesis of the main models for growth rate as a function of temperature (see also section 3.1). E, empirical models. M, mechanistic models. SE, semi-empirical models. ‘Validation’ corresponds to the original data sets used to develop and validate the models.

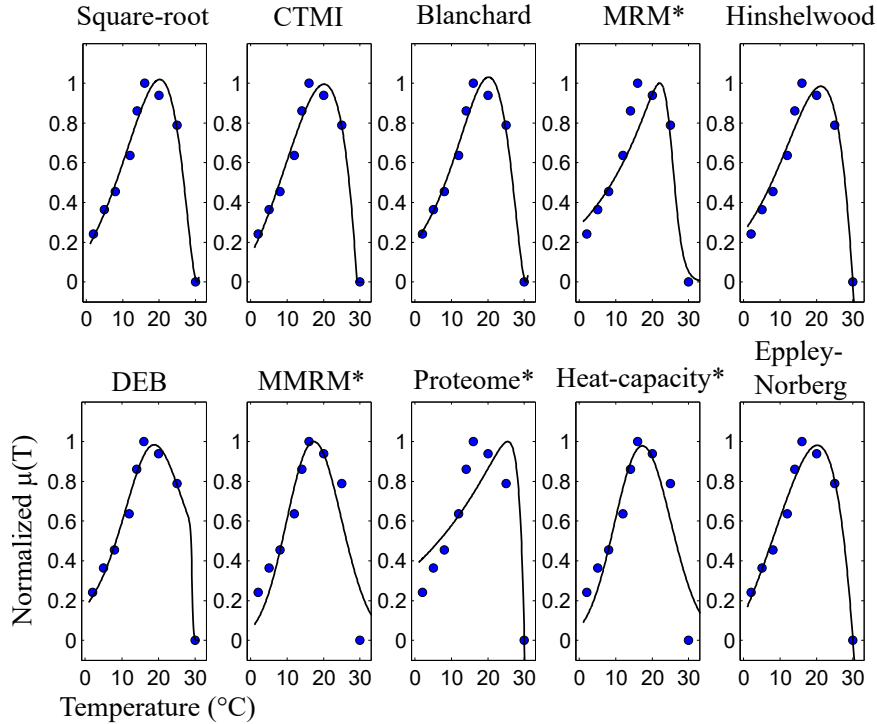


Fig. 2 Fit of the 10 described models on the normalized thermal growth curve of *Asterionella formosa* (extracted from Bernard and Rémond (2012)). Models denoted with a * are normalized. MRM, Master Reaction Model, MMRM, Modified Master Reaction Model.

Model	Calibration	r^2	AIC	BIC	# Citations
Empirical models					
Square-root	****	0.987	50.694	49.906	710
CTMI	*****	0.989	52.541	51.752	267
Blanchard	****	0.988	50.092	49.303	111
Bernard&Rémond	*****	0.989	52.541	51.752	77
Eppley-Norberg	****	0.988	52.064	51.275	146
Semi-empirical models					
Arrhenius equation	-	-	-	-	-
General mechanistic models					
Master reaction	***	0.944	33.443	32.457	107
Hinshelwood	**	0.945	37.946	37.157	507
DEB theory	*	0.985	33.748	32.368	-
Protein-stability based models					
Modified Master reaction	***	0.841	26.403	25.417	20
Proteome based	**	0.839	30.064	29.472	126
Heat capacity based	**	0.841	26.429	25.443	42

Table 2 Comparison of the main models for growth rate as a function of temperature (see also section 3.1). r^2 , |AIC| (Akaike Information Criterion) and |BIC| (Bayesian Information Criterion) are the absolute values calculated for fig. 2. ‘Calibration’ corresponds to calibration easiness, rated from 1 to 5 stars (the latter being better); calibration easiness is determined using several criteria: the associated computing time, the existence of a dedicated algorithm, the identifiability of the model, the biological meanings of the parameters. The number of citations is estimated using Google Scholar citations for the first article presenting the model.

2 Modeling the specific growth rate of unicellular organisms as a function of temperature: the thermal growth curve

40 In this section, we detail the existing models dedicated to the effect of temperature on the specific
 41 growth rate of microorganisms in non-limiting conditions (see table 1 and 2 for a summary). As
 42 discussed latter on, the specific growth rate concept (*i.e.* biomass increase per unit of time per unit
 43 of biomass) is highly dependent on the biomass descriptor.

2.1 Experimental and methodological clarifications

44 The specific growth rate is defined, in batch acclimated cultures, as the specific biomass growth
 45 rate during the exponential phase:

$$\mu(T) = \frac{1}{X} \frac{dX}{dt} = \frac{\ln(2)}{g(T)} \quad (1)$$

46 where T is a fixed temperature, X is the biomass concentration and $g(T)$ is the generation time
 47 (*i.e.* the time it takes to double the population size). The organisms are assumed to be in balanced
 48 growth conditions as defined by Campbell (1957) (*i.e.* every extensive property of the growing
 49 system increases by the same factor over a time interval), for a period long enough so that the
 50 acclimation processes have reached their steady state. $\mu(T)$ is commonly called the thermal growth
 51 curve or the thermal reaction norm (Kingsolver, 2009).

52 It is important to note that in practice the thermal growth curve depends on different factors,
 53 especially the way biomass is measured. Firstly, different biomass descriptors are commonly used,
 54 such as cell counts, particulate organic carbon concentration (POC), total cell biovolume or optical
 55 density. The dynamics of some descriptors is likely to be affected differentially by temperature
 56 than, for example, the dynamics of cell concentration. In phytoplankton, the chlorophyll content
 57 is a function of temperature (Geider, 1987), and thus the evolution of optical density results both
 58 from the growth process and from the shift in the cellular optical properties. An ideal biomass
 59 estimate should be proportional to the carbon mass with a temperature-independent constant.
 60 The difficulty to compare observations from different studies is inherent to heterogeneity in the
 61 measured descriptors.

62 Secondly, the experimental protocols are most of the time unclear on the acclimation period
 63 preceding the growth measurement. Acclimation time can vary from one day to several weeks
 64 (Boyd et al, 2013; Corkrey et al, 2014). In some cases, biomass evolution is probably affected
 65 by acclimation to the new temperature. For example, some experimental protocols proceed by
 66 gradually increasing temperature and measuring the growth rate. The main advantage is that they
 67 provides a rapid evaluation of the temperature response, but the recorded response reflects a mix
 68 between a transient acclimation phase and the effect of temperature on the cell metabolism. The
 69 possible bias is however even stronger when the descriptor used is related to carbon content with
 70 a temperature-dependent constant. For example, a too short period of acclimation results in a still
 71 evolving biomass to chlorophyll a ratio. Therefore, if the growth rate is estimated using chlorophyll
 72 a concentration (or turbidity) the computed growth rate will be biased.

73 The growth rate estimated from oxygen production must also be considered with care. The light
 74 phase of photosynthesis is mainly a photochemical process and is hardly affected by temperature at
 75 temperatures below T_{opt} . Carbon dioxide fixation in the Calvin cycle is an enzymatic process which
 76 is highly temperature dependant. Estimating growth rate from oxygen production will thus mask
 77 most of the temperature impact if an acclimation period has not been considered. The experimental
 78 acclimation period at a given temperature is of major importance for the consistency of the thermal
 79 growth curve.

80 For all these reasons, Boyd et al (2013) have developed a protocol to construct the thermal
 81 growth curve for phytoplankton and optimize the comparability of different thermal growth curves
 82 between different experiments and different species. This protocol specifies that:

- 83 1. the population must be acclimated to the experimental temperature for at least 4 generations
 84 (we recommend even 7 generations),
- 85 2. the population must be kept at an exponential growth phase using semi-continuous cultures,

- 86 3. multiple biomass descriptors must be used and compared to obtain growth rates (cell counts,
 87 chlorophyll a fluorescence, etc.); we recommend to consider carbon or dry weight for biomass,
 88 4. a minimum of 6 experimental growth rates at 6 different temperatures must be obtained,
 89 5. the cultures must be carried out with three replicates,
 90 6. all the other parameters must be kept constant, if possible at optimal levels,
 91 7. the experiments with temperatures at which the cells do not grow or grow very slowly must be
 92 repeated several times,
 93 8. several strains of the same species should be compared.

2.2 Empirical approach to model the thermal growth curve

94 Various empirical models (*i.e.* not developed from biological assumptions) have been proposed
 95 since the 1960's to represent the thermal growth curve, but only three are still commonly used.
 96 Historically, these models have mostly been developed for food-processing industry and medical
 97 applications.

98 **The Square-Root model:** The Square-Root model was initially proposed by David Ratkowsky
 99 as an alternative to the Arrhenius model (Ratkowsky et al, 1982) (see eq. 9) and then extended to
 100 the whole biokinetic range (Ratkowsky et al, 1983):

$$\mu(T) = \left[b \left(T - T_{min} \right) \left(1 - e^{c(T - T_{max})} \right) \right]^2 \quad (2)$$

101 with

$$T_{min} \leq T \leq T_{max} \quad (3)$$

102 where T_{min} and T_{max} are the minimal and maximal temperatures for growth, b is the regression
 103 coefficient of the squared root growth rate plotted against temperatures below the optimal tem-
 104 perature, and c is an additional parameter to represent growth rate decrease above the optimal
 105 temperature.

106 **The CTMI model:** The CTMI (Cardinal Temperature Model with Inflexion) was developed by
 107 Lobry et al (1991) and later popularized by Rosso et al (1993):

$$\begin{cases} \mu(T) = 0 & \text{if } T < T_{min} \\ \mu(T) = \mu_{opt} \phi(T) & \text{if } T_{min} \leq T \leq T_{max} \\ \mu(T) = 0 & \text{if } T > T_{max} \end{cases} \quad (4)$$

108 with

$$\phi(T) = \frac{(T - T_{max})(T - T_{min})^2}{(T_{opt} - T_{min}) \left[(T_{opt} - T_{min})(T - T_{opt}) - (T_{opt} - T_{max})(T_{opt} + T_{min} - 2T) \right]} \quad (5)$$

109 under the condition (Bernard and Rémond, 2012):

$$T_{opt} > \frac{T_{min} + T_{max}}{2} \quad (6)$$

110 T_{min} , T_{opt} , T_{max} are the minimal, optimal and maximal temperature for growth and μ_{opt} is the
 111 growth rate at T_{opt} . The model parameters have a direct biological interpretation. The model was
 112 built for an easy calibration on experimental data.

113 **The Blanchard model:** The Blanchard model was developed by Blanchard et al (1996) to model
 114 the photosynthetic capacity of benthic phytoplankton as a function of temperature. This model
 115 can be used to represent the thermal growth curve:

$$\mu(T) = \mu_{opt} \left(\frac{T_{max} - T}{T_{max} - T_{opt}} \right)^\beta e^{-\beta(T_{opt} - T)/(T_{max} - T_{opt})} \quad (7)$$

116 with $T \leq T_{max}$ and $T_{opt} < T_{max}$. Parameters T_{opt} and T_{max} correspond to the cardinal tempera-
 117 tures, μ_{opt} is the growth rate at $T = T_{opt}$ and β is a dimensionless parameter.

118 **The Eppley-Norberg model:** In 1972, Eppley (1972) reviewed the effect of temperature on
 119 phytoplankton growth in the sea by comparing different thermal growth curves for a variety of

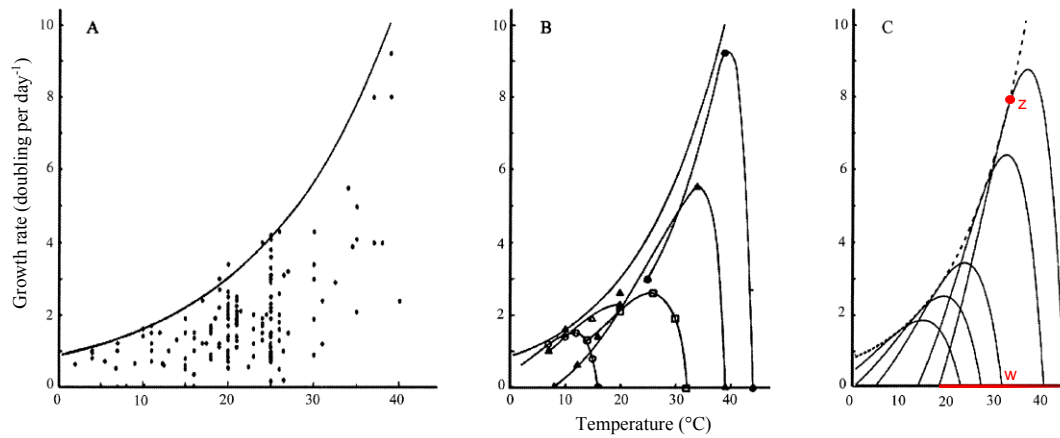


Fig. 3 A, Eppley envelope function with the original data points. B, 5 data sets for eukaryotic phytoplankton species. C, Eppley-Norberg plot for the 5 species (redrawn from Norberg (2004)).

120 phytoplankton species in non-limiting conditions (nearly 200 data points). Eppley (1972) deter-
 121 mined that the maximal growth rate μ_{opt} for each species is constrained by a virtual envelope along
 122 the optimal temperature trait T_{opt} , the so-called ‘Eppley curve’ (see fig. 3). Eppley (1972) stated
 123 that for any phytoplankton species growing under 40°C, ‘hotter is faster’.

124 Using Eppley’s hypothesis, Norberg (2004) developed a temperature-growth model, the ‘Eppley-
 125 Norberg’ model:

$$\mu(T) = \left[1 - \left(\frac{T - z}{w} \right)^2 \right] a e^{bT} \quad (8)$$

126 where w is the thermal niche width, z is the temperature at which the growth rate is equal to
 127 the Eppley function and is a proxy of T_{opt} , a and b are parameters of the Eppley function. The
 128 Eppley-Norberg model is widely used by the scientific community working on phytoplankton (*e.g.*
 129 see the recent paper of Taucher et al (2015)).

130 2.3 Empirical model comparison

131 A comparison between the Square-Root model and the CTMI was made by Rosso et al (1993) and
 132 more recently by Valik et al (2013). According to these studies, the two models fit equally well
 133 the data. Both models are validated by Valik et al (2013) using an F-test. However, the b and c
 134 parameters of the Square-root model are correlated, whereas the CTMI parameters are not, which
 135 allows easier parameter identification.

136 A more extensive comparison between the set of empirical models is presented on Figure 2
 137 for *Asterionella formosa*. It turns out that most of them can successfully describe this data set,
 138 but the fit is almost perfect for the CTMI and the Square-Root model. The CTMI proves useful
 139 for cardinal temperatures identification since all these parameters have a biological meaning. A
 140 guideline for choosing the most appropriate model is proposed in the discussion section.

141 2.4 Semi-empirical approach

142 Semi-empirical models use a combination of biological mechanisms and empirical formulations. The
 143 very first temperature model, the Arrhenius equation, was developed in this way.

144 **The Arrhenius equation:** In the beginning of the 20th century, the work of Jacobius Van't-
 145 Hoff and Svante Arrhenius on the effect of temperature on chemical reactions (Arrhenius, 1889)
 146 was introduced in biology by Charles Snyder (Snyder, 1906), setting that temperature has an
 147 exponential influence on biological reactions and then on cellular growth according to the following
 148 equation called ‘the Arrhenius law’:

$$k(T) = Ae^{-E/(RT)} \quad (9)$$

149 where $k(T)$ is the rate of reaction, R is the gas constant, A is called the ‘collision factor’ or the
 150 pre-exponential part and E is the activation energy, determined empirically. The Arrhenius equa-
 151 tion is semi-empirical, partially based on thermodynamical considerations; it can be interpreted
 152 as the number of collisions per unit of time multiplied by the probability that a collision results
 153 in a reaction. The Arrhenius equation is widely used to describe the temperature effect on differ-
 154 ent biological processes, from enzyme catalysis to community activity (*e.g.* see Frauenfelder et al
 155 (1991), Lloyd and Taylor (1994), Gillooly et al (2001)). However, it is only valid on a small range
 156 of temperature, excluding high temperatures inhibiting growth (Slator, 1916). Arrhenius model
 157 parameters are easy to estimate using an Arrhenius plot, by expressing $\ln(\mu(T))$ as a function of
 158 $1/T$, which gives a linear relationship; parameters can thus be obtained with a linear regression.
 159 The Arrhenius model allows good representations of growth rates at low temperatures, but some
 160 Arrhenius plot does not give straight lines, indicating for example that E can vary with T . More-
 161 over, the Arrhenius model cannot represent the decreasing part of the thermal growth curve, *e.g.*
 162 when temperature causes cell death. Arrhenius equation can be conveniently reformulated as:

$$k(T) = k_r e^{T_A/T_r - T_A/T} \quad (10)$$

163 where T_r is a reference temperature, T_A is the Arrhenius temperature (*i.e.* slope of the straight
 164 line of the Arrhenius plot) and k_r is the reaction rate at T_r .

165 2.5 Mechanistic approach

166 The empirical models are convenient to identify the main characteristics of the thermal growth
 167 curve. However, the mechanistic approach aims to represent the thermal growth curve as a result of
 168 the inherent physiological processes. These models are mostly based on the Arrhenius formulation,
 169 but also on the Eyring equation. In addition to their explanatory role, because their parameters
 170 have thermodynamical meanings, it is possible to extract thermodynamical informations from the
 171 thermal growth curve only.

172 2.5.1 General models based on the Arrhenius and Eyring formulations

173 **The Eyring equation and the Transition-State theory:** this theory stipulates that, during a
 174 chemical reaction, there exists an intermediate form between the reactants and the products (*e.g.*
 175 the native and denatured protein and enzyme) which is in rapid equilibrium with the reactants
 176 (Eyring, 1935):



177 where, in this example, P_f and P_u are the fraction of native and denatured proteins, respectively,
 178 and TS is the transition state. The Eyring equation, roughly similar to the Arrhenius law, was
 179 nonetheless based on these pure mechanistic considerations and reads (Eyring, 1935):

$$k(T) = \frac{K_B T}{h} e^{\Delta S^\ddagger/R} e^{-\Delta H^\ddagger/(RT)} \quad (12)$$

180 where K_B is the Boltzmann constant, h is the Planck’s constant. The parameters ΔS^\ddagger and ΔH^\ddagger
 181 correspond to the entropy and enthalpy of activation for the transition state.

182 **The master reaction model:** In 1946, Johnson and Lewin noticed that cultures of *Escherichia*
 183 *coli* exposed to 45°C during a long time ceased to grow, but grew exponentially again when replaced
 184 at 37°C. The longer the cultures were exposed to the high temperature, the lower was the growth
 185 rate at 37°C. However, there was no sign of viability loss. They concluded that cells endured
 186 reversible damage, particularly protein denaturation. They considered a simple case where a single
 187 reaction controlled by one master enzyme E_n limits growth (with no substrate limitation):

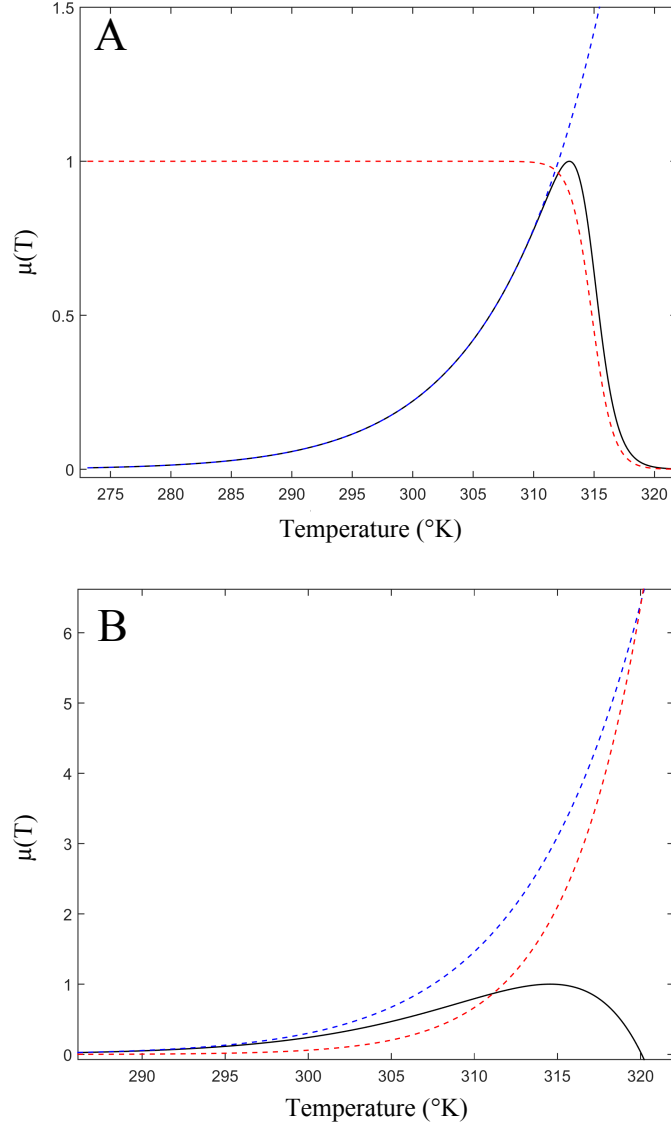


Fig. 4 Illustration of the master reaction model (A) and of the Hinshelwood model (B). The black lines correspond to $\mu(T)$, the blue dashed lines corresponds to $CTe^{-\Delta H_A^\ddagger/(RT)}$ (A) and to $f_1(T)$ (B), the red dashed line corresponds to $P(T)$ (A) and to $f_2(T)$ (B).

$$\mu(T) = cTE_n e^{-\Delta H_A^\ddagger/(RT)} e^{\Delta S_A^\ddagger/R} \quad (13)$$

188 where c is a constant given by the Eyring formulation (Eyring, 1935), ΔH_A^\ddagger is the enthalpy of
 189 activation (enthalpy difference between the transition complex and the active form) and ΔS_A^\ddagger is
 190 the entropy of activation.

191 The enzyme goes from a native, active form E_n to a reversibly denatured, inactive form E_d :



192 The chemical equilibrium is defined as:

$$K = k_1/k_2 = E_d/E_n = e^{-\Delta H/(RT)+\Delta S/R} \quad (15)$$

193 where ΔH is the enthalpy difference between the active form and the inactive form, ΔS is the
 194 entropy difference. If E_0 is the total amount of enzyme, $E_0 = E_n + E_d$. It follows that:

$$E_n = \frac{E_0}{1+K} = \frac{E_0}{1+e^{-\Delta H/(RT)+\Delta S/R}} \quad (16)$$

195 Then, by posing $C = ce^{\Delta S_A^\ddagger/R} E_0$ and replacing E_n by eq. 16 in eq. 13, Johnson and Lewin obtained
 196 the master reaction model (see fig. 4 A):

$$\mu(T) = CT e^{-\Delta H_A^\ddagger/(RT)} \cdot \underbrace{\frac{1}{1 + e^{-\Delta G(T)/(RT)}}}_{P(T)} \quad (17)$$

197 where $P(T)$ is the probability that the enzyme is in its native state and $\Delta G(T)$ is the Gibbs free
 198 energy change:

$$\Delta G(T) = \Delta H - T\Delta S \quad (18)$$

199 However, the master reaction model assumes that ΔG is temperature independent. An other version
 200 of eq.17 exists, where the exponential part does not follow an Eyring formulation but rather an
 201 Arrhenius one, which is relevant in the case of reactions with high activation energy like protein
 202 denaturation (Bischof and He, 2005):

$$\mu(T) = C e^{-\Delta H_A^\ddagger/(RT)} \cdot \frac{1}{1 + e^{-\Delta G(T)/(RT)}} \quad (19)$$

203 It is worth noting that this equation here simplifies the calculation of the cardinal temperature
 204 T_{opt} and is supposed to have little influence on the model fit and behavior (see table 1 and 2).

205 **The Hinshelwood model:** In 1945, Sir Norman Hinshelwood proposed a rather simple model in
 206 which the temperature-dependent growth rate is just the difference between a synthesis rate $f_1(T)$
 207 and a degenerative rate $f_2(T)$ (Hinshelwood, 1945) (see fig. 4 B):

$$\mu(T) = \underbrace{A_1 e^{-E_1/(RT)}}_{f_1(T)} - \underbrace{A_2 e^{-E_2/(RT)}}_{f_2(T)} \quad (20)$$

208 where A_1 and A_2 are related to entropy and E_1 and E_2 are related to enthalpy. Hinshelwood
 209 believed that the function $f_2(T)$, which causes the ‘catastrophic decline to zero’(Hinshelwood,
 210 1945), represents protein denaturation. He argued that the model only works if E_2 is higher than E_1 ,
 211 because the degenerative process represented by $f_2(T)$ must be sudden. Since protein denaturation
 212 possesses a high activation energy, it is a good candidate for driving the process. Moreover, A_2
 213 (corresponding to entropy) also has to be quite high. Thus, the ‘activated state must be highly
 214 disordered compared with the initial state’ which ‘results in an easy transition to the activated state
 215 in spite of the large amount of energy which has to be taken up to reach it’(Hinshelwood, 1945).
 216 Precisely, protein denaturation leads from a highly ordered state to an highly disordered state and
 217 is therefore associated with a large entropy increase. From the Hinshelwood model, after some
 218 mathematical manipulations, it is possible to express T_{min} , T_{opt} , T_{max} (see table 1).

219 **The DEB theory approach:** In the Dynamics Budget Theory, the effect of temperature on
 220 population growth is taken into account using a modified Master Reaction model (Kooijman,
 221 2010), where all the temperature-dependent functions are Arrhenius modified equations:

$$\mu(T) = \frac{k_1 e^{T_A/T_1 - T_A/T}}{\underbrace{1 + e^{T_{AL}/T - T_{AL}/T_L} + e^{T_{AH}/T_H - T_{AH}/T}}_{f_D}} \quad (21)$$

222 where T_L and T_H are related to cold and hot denaturation (lower and upper boundaries), T_{AL} and
 223 T_{AH} are the Arrhenius temperatures (*i.e.* the slope of the straight line of the Arrhenius plot at
 224 low and high temperatures respectively, see eq. 10). The ratio f_D^{-1} corresponds to the fraction of
 225 enzyme in its native state. This model therefore also accounts for cold denaturation, contrary to
 226 the Master Reaction model.

227 2.5.2 The protein thermal stability hypothesis

228 In addition to the temperature-dependent enzyme activity, protein thermal stability plays a key role
 229 in the microbial thermal growth curve (Johnson and Lewin, 1946; Rosenberg et al, 1971; Zeldovich
 230 et al, 2007; Pena et al, 2010). If temperature increases, certain proteins become first inactive and
 231 then denatured. Especially, at high temperatures ($T > T_{opt}$), this phenomenon occurs for many
 232 proteins and causes a growth rate decrease. In line with the master reaction model, some models

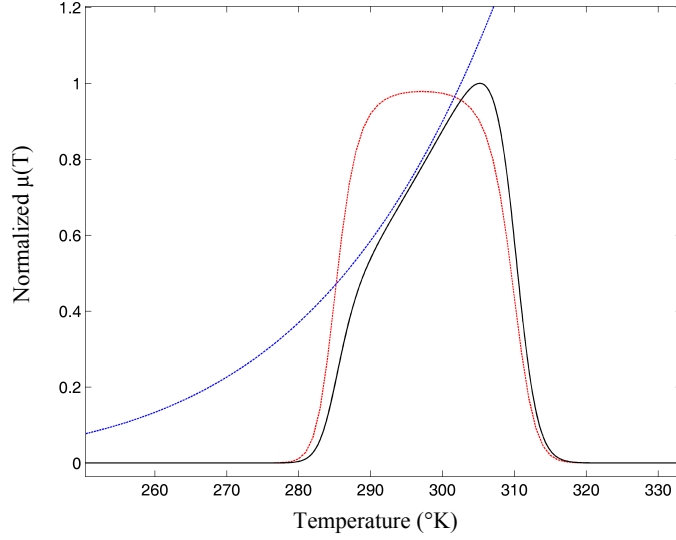


Fig. 5 The modified master reaction model plot for a microbial species (black line) with activation function (blue dashed line) and protein denaturation probability $P(T)$ (red dashed line).

233 include additional assumptions about protein thermal stability and its consequences on growth,
 234 assuming that proteins are the key factors controlling thermal growth curves.

235 **The modified master reaction model:** The master reaction model assumes that ΔG , the
 236 Gibbs free energy difference between the native and denatured protein, is temperature independent.
 237 Based on Murphy et al (1990) work, Ross (1993) and then Ratkowsky et al (2005) remarked that
 238 ΔG should vary with T in eq. 17 following eq. 18. Moreover, Murphy et al (1990) showed that
 239 globular proteins (including enzymes) share common thermodynamic properties. For any protein,
 240 the denaturation enthalpy change (ΔH) and the denaturation entropy change (ΔS), normalized to
 241 the number of amino-acids residues of this protein, both converge to a fixed value ΔH^* and ΔS^*
 242 at T_H^* and T_S^* respectively (Privalov, 1979). The reason for such a temperature convergence is still
 243 unclear. Nonetheless, it has been shown that, at T_H^* and T_S^* , the hydrophobic contribution to ΔH
 244 and ΔS approaches zero (Robertson and Murphy, 1997). Using the heat capacity thermodynamic
 245 parameter C_p , Murphy et al (1990) stated that ΔH and ΔS can be expressed as a function of the
 246 heat capacity change ΔC_p :

$$\Delta H = \Delta H^* + \Delta C_p(T - T_H^*) \quad (22)$$

$$\Delta S = \Delta S^* + \Delta C_p \ln(T/T_S^*) \quad (23)$$

247 where ΔH^* is the enthalpy change per mol of amino-acid residue of the enzyme at T_H^* , ΔS^* is
 248 the entropy change per mol of amino-acid residue of the enzyme at T_S^* , ΔC_p is the heat capacity
 249 difference between the native and denatured protein, T_H^* is the temperature at which the contri-
 250 bution of ΔC_p to enthalpy is zero and T_S^* is the temperature at which the contribution of ΔC_p
 251 to entropy is zero. The heat capacity change ΔC_p is constant for a given protein (Privalov and
 252 Khechinashvili, 1974). Using eq. 22 and eq. 23, the Gibbs free energy of protein denaturation (*i.e.*
 253 the protein thermal stability) is (fig. 5):

$$\Delta G(T) = n \left[\Delta H^* - T \Delta S^* + \overbrace{\Delta C_p [(T - T_H^*) - T \ln(T/T_S^*)]}^{\Delta G_{hydro}} \right] \quad (24)$$

254 where n is the number of amino-acid residues in the master enzyme and ΔG_{hydro} is the hydrophobic
 255 contribution to the free energy change. Eq. 24 describes protein thermal stability in terms of
 256 hydrophobic contribution of apolar compounds.

257 Ross (1993) and Ratkowsky et al (2005) proposed to replace ΔG by eq. 24 in eq. 17 (forming the
 258 modified master reaction model). Because T_H^* , T_S^* and ΔS^* are considered as universal constant
 259 for globular proteins (Murphy and Gill, 1991), the modified master reaction model has 5 tunable

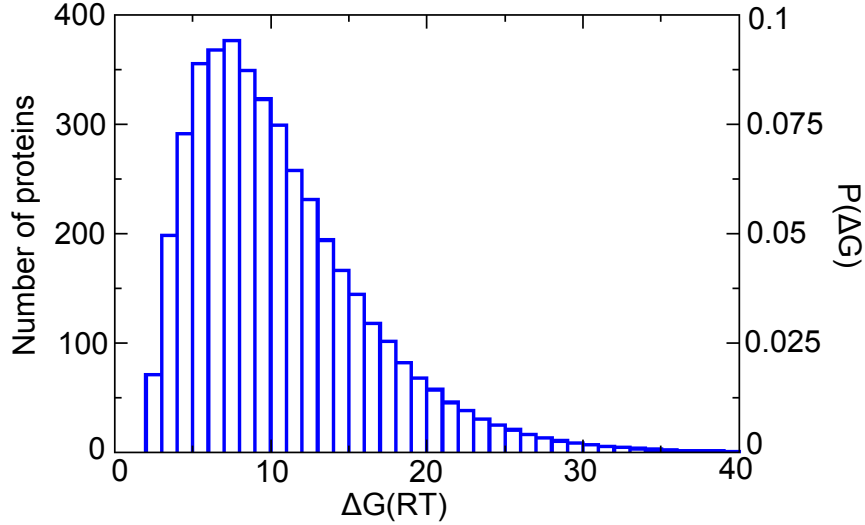


Fig. 6 Gibbs free energy distribution of *Escherichia coli* proteome at 37°C (adapted from Ghosh and Dill (2010)).

parameters (fig. 5). As a validation, Ratkowsky et al (2005) fitted the model on 35 bacterial strains normalized data sets obtained in non-limiting conditions. Their main conclusion points towards the crucial role played by a single master enzyme whose thermal sensitivity is driven by hydrophobic interactions.

Corkrey et al (2014) extended the modified master reaction model to unicellular and multicellular eukaryotes. They considered ΔH^* as a universal constant as well, reducing the model parameters to 4. They fitted the model on 230 strains normalized data sets covering a range of 124°C. Their principal conclusion states that the model is able to find coherent protein thermodynamics parameters with only net growth rates data (*i.e.* growth rate versus temperature). Hyperthermophiles proteins seem to be more widely robust. Moreover, they found several links between thermodynamic parameters, for example between T_{opt} and ΔC_p (enzyme stability), and between T_{opt} and ΔH^\ddagger (enzyme activity). However, they did not provide further explanations. They finally speculate on the nature of the single limiting reaction. They assume that if a single reaction (and not several) is rate limiting, then it should be linked to the protein unfolding and re-folding process. They particularly focus on the role of chaperones proteins responsible for *de novo* folding.

The proteome-scale approach: Zeldovich et al (2007) proposed that the whole proteome plays a role in microbial thermal sensitivity. Resuming this idea, Chen and Shakhnovich (2010) considered that each important protein i has its own Gibbs free energy of denaturation ΔG_i . The growth rate of a microbe becomes dependent of the stability of each protein, and the thermal denaturation of several proteins causes a bottleneck effect on growth:

$$\mu(T) = CT e^{-\Delta H^\ddagger/(RT)} \cdot \frac{1}{\prod_i^{N_p} (1 + e^{-\Delta G_i(T)/(RT)}} \quad (25)$$

where N_p is the number of proteins. According to Zeldovich et al (2007), the proteome can be described in protein stability distribution thanks to a dedicated probability function of the Gibbs free energy, $P(\Delta G)$ (see fig.6). By taking the natural logarithm of eq. 25, Chen and Shakhnovich (2010) expressed the growth rate as:

$$\ln(\mu(T)) = \ln(CT) - \Delta H^\ddagger/(RT) - \sum_{i=1}^{N_p} \ln(1 + e^{-\Delta G_i/(RT)}) \quad (26)$$

that is, by integrating the resulting equation over the whole $P(\Delta G)$ distribution range and by averaging over the proteome:

$$\ln(\mu(T)) \simeq \ln(CT) - \Delta H^\ddagger/(RT) - N_p \int_0^L \ln\left(1 + e^{-\Delta G/(RT)}\right) P(\Delta G) d\Delta G \quad (27)$$

287 where L is the maximum value of ΔG (for example $L = 40$ in fig. 6). N_p can be reduced to the
 288 number of the only important proteins. According to Sawle and Ghosh (2011) and Ghosh and Dill
 289 (2010), ΔG can be expressed as a function of ΔH , ΔS and ΔC_p (using eq. 22 and eq. 23), itself
 290 depending on the protein chain length denoted N :

$$\Delta G = \Delta H(N) + \Delta C_p(N)(T - T_h) - T\Delta S(N) - T\Delta C_p(N)\ln(T/T_s) \quad (28)$$

291 with

$$\begin{aligned} \Delta H(N) &= aN + b \\ \Delta S(N) &= cN + d \\ \Delta C_p(N) &= lN + m \end{aligned} \quad (29)$$

292 where a, b, c, d, l, m are empirical parameters defined for mesophilic and for thermophilic organisms.
 293 The distribution of chain length over the proteome $P(N)$ can be known (Zhang, 2000) and is used
 294 to estimate $P(\Delta G)$. It can be modelled by a gamma distribution:

$$P(N) = \frac{N^{\alpha-1} e^{-N/\theta}}{\Gamma(\alpha)\theta^\alpha} \quad (30)$$

295 where θ and α are the parameters of the gamma distribution corresponding to:

$$\begin{aligned} \langle N \rangle &= \alpha\theta \\ \langle (\Delta N)^2 \rangle &= \alpha\theta^2 \end{aligned} \quad (31)$$

296 The brackets represent the mean over all the proteins. $\Gamma(\alpha)$ is the gamma function evaluated at
 297 α . The model (eq. 27), presented as universal, has thus only two parameters, N_p and ΔH^\ddagger . It has
 298 been validated on 12 normalized data sets of prokaryotes.

299 **The heat capacity hypothesis:** Hobbs et al (2013) and Schipper et al (2014) proposed a
 300 model called the Macromolecular Rate Theory (MMRT) in which the thermal growth curve is
 301 driven by the heat capacity change of activation ΔC_p^\ddagger (*i.e.* the heat capacity difference between
 302 the ground state and the transition state). More precisely, the growth rate is expressed as:

$$\mu(T) = \frac{k_B}{h} T e^{\Delta G^\ddagger(T)/(RT)} \quad (32)$$

303 where k_B and h are the Boltzmann and Planck's constants, ΔG^\ddagger is the Gibbs free energy difference
 304 between the ground state and the transition state of a possible rate-limiting enzyme. Contrary to
 305 the master reaction model, the MMRT considers that enzymes do not denature easily and are in
 306 rapid equilibrium with a folded, inactive intermediate (*i.e.* the transition state). The Gibbs free
 307 energy difference can be here written as:

$$\Delta G^\ddagger(T) = \Delta H_{T_0}^\ddagger + \Delta C_p^\ddagger(T - T_0) + T(\Delta S_{T_0}^\ddagger + \Delta C_p^\ddagger \ln(T/T_0)) \quad (33)$$

308 If $\Delta C_p^\ddagger > 0$, then the heat capacity difference between the ground state and the transition state
 309 (*i.e.* the inactive folded enzyme) itself is sufficient to explain the decrease of growth rate above
 310 T_{opt} . Schipper et al (2014) validated the MMRT model on microbial soil processes data sets.

311 2.6 Mortality induced by temperature

312 Warm temperatures increase cell mortality because of protein denaturation and membranes in-
 313 juries. For phytoplankton, photosystems and electron chain transport are denaturated (Song et al,
 314 2014), and a transient imbalance between the energy needed and produced must be managed by
 315 the cell (Ras et al, 2013; Smelt and Brul, 2014; Serra-Maia et al, 2016).

316 So far, models explicitly presenting the mortality rate as a function of temperature are rare.
 317 The Hinshelwood model explicitly integrates a mortality rate with an Arrhenius law (see fig. 7 B).
 318 This model turned out to efficiently represent mortality together with growth for the chlorophyta
 319 *Chlorella vulgaris* (Serra-Maia et al, 2016). Another example is Van Uden (1985) who combined a
 320 master reaction growth model and an exponential death model for yeast:

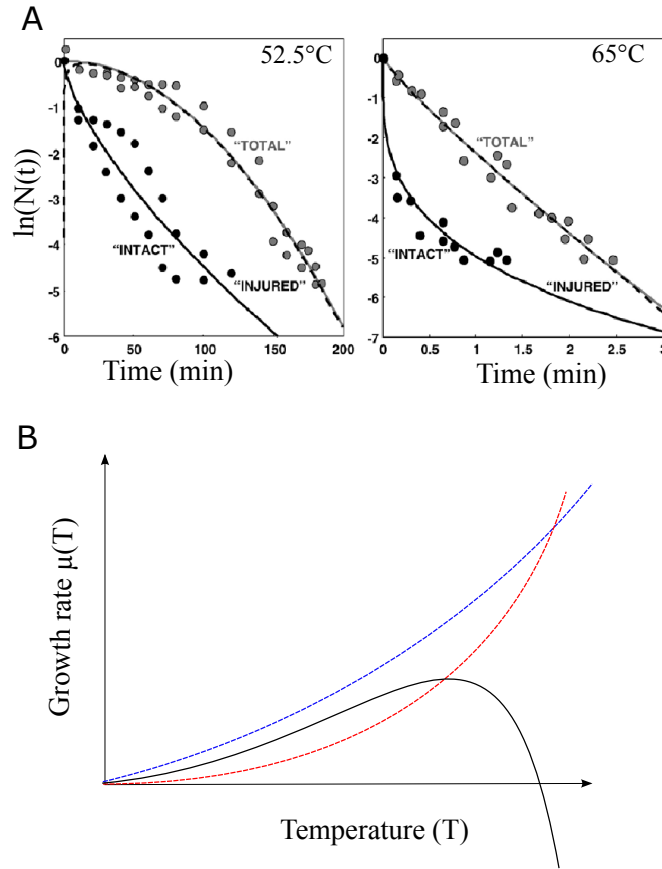


Fig. 7 A, Survival curves at different temperatures for *Listeria innocua* (redrawn from Corradini and Peleg (2006)). B, Hinshelwood model (black curve) with mortality (red curve) as in Serra-Maia et al (2016).

$$\mu(T) = \frac{C e^{-\Delta H^\ddagger/(RT)}}{1 + e^{-\Delta G/(RT)}} - \frac{k_B T}{h} e^{\Delta S_{den}^\ddagger/R - \Delta H_{den}^\ddagger/(RT)} \quad (34)$$

321 where ΔS_{den}^\ddagger and ΔH_{den}^\ddagger are the entropy and enthalpy of activation of cells mortality.

322 Outside of the thermal niche width, for temperatures above the species T_{max} , the kinetics of
 323 cell inactivation is called the survival curve (Moats, 1971) (fig. 7 A); from each survival curve, it is
 324 possible to infer the mortality rate at a given temperature. Different empirical models have been
 325 developed, especially in food science, to represent these survival curves (Mafart et al, 2002; Smelt
 326 et al, 2002; Smelt and Brul, 2014).

327 3 Choosing the most appropriate model

328 In this section, we propose a guideline for choosing the most appropriate model depending on the
 329 study objectives. We summarize and compare the models performance and their applicability to
 330 phytoplankton in different modeling scenario, and highlight the most appropriate models.

331 The model comparison is based on the analysis of 193 thermal curve responses associated to
 332 193 different strains, resulting from 130 species (Thomas et al, 2012). This data set includes the
 333 main phyla of unicellular photosynthetic organisms.

334 An illustration of the model performance for 5 strains of the cyanobacterium genus *Synechococ-*
 335 *cus* sp. is plotted on fig. S1 (Pittera et al, 2014).

3.1 Synthesis of model performance

Three criteria have been considered to assess a model efficiency. The absolute model performance is estimated using r^2 . To account both for the fit quality and the number of parameters, we considered the Akaike Information Criterion (AIC) (Akaike, 1992) and the Bayesian Information Criterion (BIC) (Schwarz et al, 1978) (see table 2 and table S1-S3). The best models are, globally, the empirical models, and the CTMI and the Eppley-Norberg turn out to obtain the best score (see table S2, fig. S2). The Hinshelwood model, in the other way, has the best score among the mechanistic models. It is worth noting here that the CTMI assumes that $T_{max} - T_{opt} \leq T_{opt} - T_{min}$, which is not the case for the Eppley-Norberg. Thus, for small data sets with few points near T_{opt} , the Eppley-Norberg model has a better fit score (see fig. S3).

To highlight the combination of fit quality and other important characteristics, we defined several criterions in table 1. From these criterions, we could derive advantages, limitations and rating for each model (table 1). The CTMI, Bernard&Rémond and the Hinshelwood model obtain the highest score, with the best trade-off between complexity (*e.g.* few parameters), fit quality, calibration easiness and parameters interpretation.

3.2 Macroscopic modeling without including mortality

A common scenario when modeling the effect of temperature on phytoplankton is the need of representing the net thermal response, without explicitly representing mortality. The response is generally focusing on growth rate, but it can also represent a detailed physiological processes. Below the optimal temperature, the Arrhenius equation has been widely used, has a good fit, is easy to calibrate and its parameters can be interpreted. However, to represent the whole thermal growth curve, the CTMI is the best choice because its parameters are directly the cardinal temperatures and its calibration is easily possible thanks to a dedicated algorithm. Other similar models (*e.g.* Eppley-Norberg) are also satisfactory. When light is not photoinhibiting, these models can be easily combined with the light effect on growth. In particular, the Bernard&Rémond model is a good trade-off. This latter model has been originally validated on 15 phytoplankton species and here on 193 phytoplankton species (table S1-S3) from the main phytoplankton phyla. The CTMI is thus expected to be the ideal candidate to represent the effect of temperature on phytoplankton communities. The Eppley-Norberg model is also interesting for modeling communities given that from its four parameters, two are considered universal and only two are strain-specific.

3.3 Macroscopic modeling with explicit mortality rate

As we pointed out, few studies exist to represent the effect of temperature on phytoplankton mortality. The only model that explicitly represents mortality is the Hinshelwood model. Adapted for phytoplankton (Serra-Maia et al, 2016), this model is thus recommended because its parameters can be interpreted, and the fit quality is acceptable; however, its parameters calibration are not easy on experimental data with few data points. We thus recommend to use the CTMI to generate a patron for the net growth rate. The patron, made of the data points simulated by the CTMI model can then be advantageously used to calibrate the Hinshelwood model.

3.4 Physiological or metabolic modeling

The proteome model is certainly the best candidate to explain the thermal growth curve, as it includes the effect of temperature on the whole proteome and has only two parameters. However, it does not fit very well the experimental data for phytoplankton growth rates compared to the empirical models. As for the Hinshelwood model, a patron can be used to artificially increase the number of data points. This model could also be adapted to phytoplankton when light is photoinhibiting.

Model	Advantages	Limitations	Rating
Square-root	Fit quality	No mortality, T_{opt} is not easily defined	***
CTMI	Fit quality, parameters interpretation	No mortality	****
Blanchard	Calibration easiness, fit quality, application to phytoplankton	No mortality T_{min} is not defined	***
Bernard&Rémond	Calibration easiness, fit quality, parameters interpretation, application to phytoplankton	No mortality	*****
Eppley-Norberg	Fit quality, application to phytoplankton	No mortality, implicit link between T_{opt} and μ_{opt}	****
Arrhenius equation	Fit quality below T_{opt}	No representation of the decreasing phase above T_{opt}	**
Master reaction	Parameters interpretation	T_{min} and T_{max} are undefined	**
Hinshelwood	Fit quality, parameters interpretation, explicit mortality	T_{min} is not defined	****
DEB theory	Fit quality	High number of parameters	*
Modified Master reaction	Parameters interpretation	Poorness of fit	**
Proteome based	Parameters interpretation, only 2 parameters	Poorness of fit	***
Heat capacity based	-	Poorness of fit, parameters interpretation not clear	*

Table 3 Advantages, limitations and rating of the main models for growth rate as a function of temperature. Rating is based on criterion from table 1, from 1 to 5 stars (the latter being better).

381 4 Coupling temperature and other environmental factors

382 4.1 Factors influencing the thermal growth curve

383 The thermal growth curve is assumed to be obtained in non-limited conditions (Kingsolver, 2009).
 384 However, some limitations and perturbations usually occur in the environment that may simultane-
 385 ously involve changes in metabolism. The simplest representation of some multi-factors impact on
 386 the growth rate is to assume that all the factors are uncoupled. A classical formalism to represent
 387 the effect of n uncoupled factors is given by the gamma concept (Zwietering et al, 1993; Augustin
 388 and Carlier, 2000):

$$\mu = \mu_{opt} \cdot \prod_{k=1}^n \gamma_k \quad (35)$$

389 where μ_{opt} is the maximal growth rate when all the n environmental factors are optimal, γ_k
 390 is a normalized function of the environmental factor k . One of the γ_k represents the impact of
 391 temperature.

392 In a more accurate approach, the impact of a factor on the cardinal temperatures can be repre-
 393 sented (or more generally the parameters of the thermal model can be a function of another factor).
 394 In this case, these environmental factors are coupled to temperature. For example, temperature
 395 plays a role on oxygen dissolution in water, and the two factors have then a coupled effect on
 396 microbial growth rates; this coupling is enhanced for unicellular diazotrophic cyanobacteria which
 397 are particularly sensitive to the oxygen concentration, because oxygen inhibits their diazotrophic
 398 activity (Brauer et al, 2013).

399 For the majority of phytoplankton species, the most important physico-chemicals factors are
 400 light and nutrients (mainly N and P) (Falkowski and Raven, 2013).

401 4.2 The interplay between light and temperature in phytoplankton

402 Phytoplankton perform oxygenic photosynthesis to harvest light. Photosynthesis metabolism is
 403 composed of a dark phase and a light phase, with different thermal sensitivities. The dark phase

404 involves the Rubisco enzyme responsible for CO₂ fixation in the Calvin cycle. In the light phase, at
 405 low temperatures, the reactions are mainly photochemical and not enzymatic and thus less sensitive
 406 to temperature. As a consequence, the cell has to balance the energy and electrons transferred from
 407 photons harvesting and their conversion into chemical energy in the dark phase, depending on the
 408 temperature (see for example the review by Ras et al (2013)). A shift down to low temperatures
 409 induces a strong imbalance and thus generates light saturating conditions (see Young et al (2015)).
 410 However, at high temperatures, the light phase is strongly affected by temperatures as electron
 411 transport chains and photosystems structural stability is affected (Song et al, 2014) and can induce
 412 cell mortality.

413 4.2.1 Models assuming an uncoupling between light and temperature effects

414 These models assume that temperature and light are independent factors. For example, the model
 415 developed by Bernard and Rémond (2012) supposes that the growth rate is expressed as:

$$\mu(T, I) = f(I) \cdot \phi(T) \quad (36)$$

416 where $\phi(T)$ corresponds to the CTMI (eq. 5) and:

$$f(I) = \mu_{max} \frac{I}{I + \frac{\mu_{max}}{\alpha} \left(\frac{I}{I_{opt}} - 1 \right)^2} \quad (37)$$

417 μ_{max} is the maximum growth rate at optimal light intensity I_{opt} and optimal temperature T_{opt} , α is
 418 the initial slope of the light response curve. $f(I)$ was built in line with the Peeters and Eilers (1978)
 419 model with photoinhibition, but reparametrized for a better parameter identification. Bernard and
 420 Rémond (2012) developed an algorithm to identify the cardinal temperature from data sets with
 421 different light conditions. This model was validated on 15 phytoplankton species. The hypothesis
 422 of uncoupling is, however, no longer available at high light intensities (*i.e.* when photoinhibition
 423 occurs) as temperature is known to play a role in photoinhibition (Jensen and Knutsen, 1993;
 424 Edwards et al, 2016).

425 The model of Eppley-Norberg modified by Follows et al (2007), uses another formalism to
 426 represent both temperature and light effect:

$$\mu(T, I) = \mu_{max} \cdot \underbrace{\frac{1}{\tau_1} \left(A^T e^{-B(T-T_0)^c} - \tau_2 \right)}_{\gamma^T} \cdot \underbrace{\frac{1}{\gamma_{max}^I} (1 - e^{-k_p I}) e^{-k_i I}}_{\gamma^I} \quad (38)$$

427 where μ_{max} is the species maximum growth rate, γ^T and γ^I are respectively the normalized tem-
 428 perature function and the normalized photosynthesis function. The parameters τ_1 and τ_2 ensure
 429 the normalization of γ^T , while parameters A , B , T_0 and c modify its shape by taking into ac-
 430 count the Eppley hypothesis (see fig.8). Similarly, γ_{max}^I ensures the normalization of γ^I , $1 - e^{-k_p I}$
 431 represents the increase of growth with light at low irradiance and k_i is a constant associated to
 432 photo-inhibition.

433 4.2.2 Models considering a coupling between light and temperature

434 The model developed by Dermoun et al (1992) for the unicellular Rhodophyta *Porphyridium cru-*
 435 *entum* accounts for a complex coupling between light and temperature:

$$\mu(T, I) = 2\mu_m(T)(1 + \beta_1) \frac{I/I_{opt}(T)}{1 + 2\beta_1 I/I_{opt}(T) + (I/I_{opt}(T))^2} \quad (39)$$

436 where $\mu_m(T)$ is the maximum specific growth rate at a given temperature T , I_{opt} is the optimal
 437 irradiance at a given temperature T and β_1 is the shape factor for limiting irradiance. $\mu_m(T)$
 438 and $I_{opt}(T)$ are rational functions (see Dermoun et al (1992)). It is worth noting that the tight
 439 coupling between light and temperature in this model leads to identifiability problems partially due
 440 to large number of parameters (9 parameters in the model). Furthermore, when light is limiting,
 441 the coupling between light and temperature becomes loose.

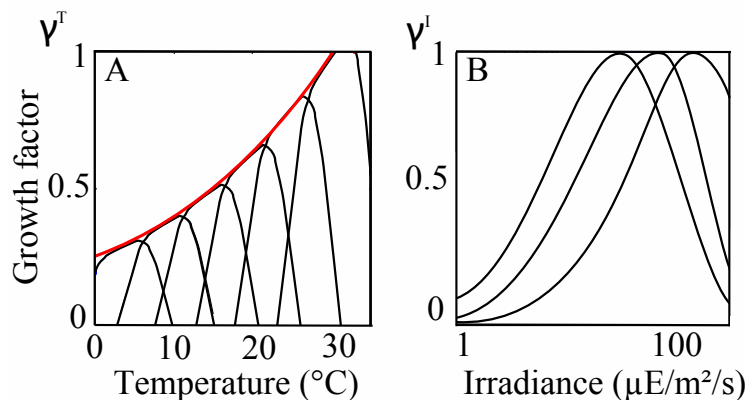


Fig. 8 A, Eppley curve normalized at 30°C . B, photosynthesis as represented in eq. 38. The figure is redrawn after Follows et al (2007).

442 4.3 The interplay between nutrients and temperature

443 Phytoplankton growth in the oceans is often limited by nitrogen (N) or phosphorus (P). When
 444 limiting, these nutrients strongly impact the thermal growth curve (Pomeroy and Wiebe, 2001;
 445 Thomas, 2013; Thomas and Litchman, 2016). Trace nutrients such as trace metals or essential
 446 vitamins can also play an important role on growth but their interplay with temperature is largely
 447 unknown.

448 Thomas (2013) has developed a model taking into account the nutrient effect (N), assuming
 449 that anabolism is temperature-dependent and nutrient-dependent, whereas catabolism or mortality
 450 only depend on temperature:

$$\mu(T, N) = b_1 e^{b_2 T} \frac{N}{N + K} - (d_1 e^{d_2 T} + d_0) \quad (40)$$

451 where b_1 , b_2 , d_1 , d_2 are Arrhenius parameters for anabolism and catabolism, respectively, and K
 452 is the half-saturation constant of a Michaelis-Menten kinetics of nutrient uptake. d_0 is a constant
 453 catabolism rate independent of temperature. Nutrient limitation leads to a decrease of the thermal
 454 niche width, T_{opt} and μ_{opt} (see fig. 9 A). The model has been validated on temperature and nutrient
 455 experiments conducted with the phytoplankton diatom species *Thalassiosira pseudonana* (Thomas
 456 et al, 2017).

457 Grimaud (2016) has developed a dynamical model taking into account temperature and nutrient
 458 for eukaryotes phytoplankton species, based on the Droop model (Droop, 1968). In balanced-growth
 459 conditions, the model gives the following thermal growth curve:

$$\mu(T, N) = \frac{\phi_2(T)\phi_1(T)\rho(N)}{\phi_1(T)\rho(N) + \phi_2(T)Q_0} - m \quad (41)$$

460 where $\phi_1(T)$ and $\phi_2(T)$ are CTMI equations for nutrients and carbon uptake, $\rho(N)$ is a normalized
 461 Michaelis-Menten equation, Q_0 corresponds to the minimal internal nutrient quota needed to grow,
 462 m is the constant mortality/catabolism rate. Fig. 9 B shows that a nutrient limitation leads to
 463 a decrease of T_{opt} and μ_{opt} , in line with Thomas (2013). However, the amplitude of the thermal
 464 niche width is less marked, and is only reduced for strong nutrient limitation (see fig. 9 B). Also,
 465 these results depend on the difference between $\phi_1(T)$ and $\phi_2(T)$.

466 5 Accounting for temperature variations

467 In the natural environment, cells experience temperature fluctuations at different time-scales, rang-
 468 ing from days to seasons, influencing their physiology and forcing them to acclimate (Ras et al,
 469 2013; van Gestel et al, 2013). The question is then how to deal with these variations, while thermal
 470 growth curves are obtained in balanced conditions.

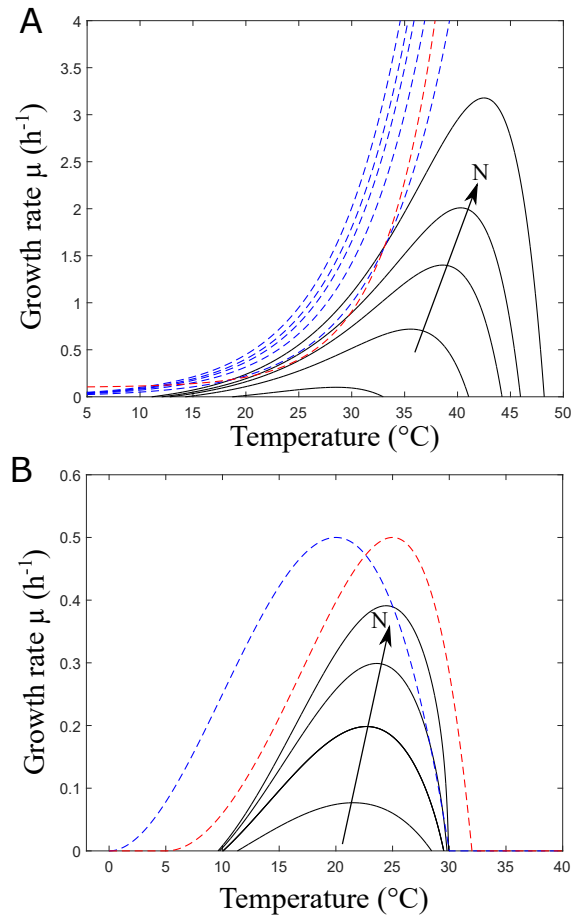


Fig. 9 Growth rate as a function of nutrient and temperature $\mu(T, N)$. The black lines correspond to different nutrient values, increasing with the arrow. A, model of Thomas (2013). The blue and red dashed lines correspond to the positive and negative terms of eq. 40, respectively. B, model of Grimaud (2016). Blue and red dashed lines correspond to $\phi_1(T)$ and $\phi_2(T)$ of eq. 41, respectively.

471 5.1 Assuming instantaneous acclimation at large time scale

472 The specific growth rate $\mu(T)$ described in section 2.1 for balanced growth has been used as such
 473 when temperature is time-varying, assuming that the effect of temperature is instantaneous (see
 474 for example Baranyi and Roberts (1995); Baranyi et al (1995)). This approximation is valid in
 475 particular for slow variations of temperature, such as annual fluctuation of sea temperature.

476 5.2 Acclimation to temperature variations

477 Cell acclimate to temperature by adjusting the biosynthesis of key components (Hall et al, 2010;
 478 Ras et al, 2013). For example, Geider (1987) showed that phytoplankton cells are able to adapt
 479 their pigment content when temperature changes. The chlorophyll concentration is adjusted to
 480 the photon flux and to the cells capacity of converting it into chemical energy. The carbon to
 481 chlorophyll ratio ($\theta = Chl_a : C$) increases with temperature, and, following Geider (1987), this
 482 ratio converges after an acclimation phase to $\theta^*(T)$:

$$\theta^*(T) = \frac{e^{kT}}{(a - bT)e^{kT} + cI} \quad (42)$$

483 where a , b , c , k are constants and I is the light intensity. However, eq. 42 is valid for balanced
 484 growth.

485 Dynamical models representing acclimation should therefore consider the different cellular com-
 486 ponents, and include the temperature effect on each reaction kinetic. Models for phytoplankton
 487 including chlorophyll have been proposed for example by Geider et al (1998), but the temperature
 488 effect has been overlooked (assuming that all the kinetics have the same temperature dependence).

489 In Bernard et al (2015), an equation for cell acclimation is proposed, which can be straightfor-
 490 wardly extended to acclimation to temperature:

$$\dot{\theta} = \delta \mu(T) [\theta^*(T) - \theta] \quad (43)$$

491 where δ is a parameter modulating the acclimation rate, which is assumed proportional to the
 492 growth rate μ . This kind of models is of particular interest given that it can deal with both
 493 temperature fluctuations and the interplay with other factors such as light, but more experimental
 494 data are required for calibration and validation.

495 6 Conclusion and future developments

496 To better picture the temperature effect, there is an urgent need for standard protocols, as proposed
 497 by Boyd et al (2013), fulfilling two crucial points: *i*/ assess the growth rate with biomass proxies
 498 which are not influenced by temperature; *ii*/ consider acclimation periods of at least one week for
 499 each temperature. Such a protocol is required to isolate the impact of temperature on growth and
 500 to compare different experimental results.

501 Despite their simplicity, empirical models turn out to be very acute for representing the exper-
 502 imental data sets for phytoplankton (see fig. 2). Nonetheless, to be efficient, these models must be
 503 associated to tailored calibration algorithms in line with Bernard and Rémond (2012) to rapidly
 504 fit a data set and quantify the uncertainty.

505 The mechanistic approach brings a complementary viewpoint in the modeling of the thermal
 506 growth curve but also in representing the temperature response for non-balanced growth conditions.
 507 Temperature plays a concurrent role on enzyme activity and therefore on reactions kinetics, and
 508 on cell structural stability. Most of the mechanistic models consider that a single enzyme controls
 509 growth at low temperatures (*e.g.* MMRM and proteome-scale approach) whereas temperature
 510 affects enzyme and protein conformational stability and leads to a decrease of growth at high
 511 temperatures (Ghosh et al, 2016). Despite the recent development of a promising unicellular growth
 512 model (Corkrey et al, 2014), this ‘proteome paradigm’ should be further investigated for several
 513 reasons. First, the effect of temperature on protein stability is still relatively unclear given that we
 514 do not know, for example, in which extent proteins denaturation proceeds the same way in vivo as in
 515 vitro (Leuenberger et al, 2017). Second, other structural components play an important role in the
 516 cell thermal stability, and especially on membrane fluidity (Caspeta et al, 2014). Third, cells have
 517 the capacity to repair their damages and regrow after a heat shock (Li and Srivastava, 2004) which is
 518 not clearly understood, as well as the molecular mechanisms protecting against mortality (Ghosh
 519 et al, 2016). Finally, the link between the mortality rate and protein denaturation still remains
 520 unclear; it is for example not known how mortality increases between T_{opt} and T_{max} . Mortality
 521 models in line with Serra-Maia et al (2016) are needed. In addition to the ‘proteome paradigm’
 522 limits, the effect of temperature on cells kinetics is not limited to one enzyme controlling growth, but
 523 apply for all reactions. Some authors, for example, claim that the thermal growth curve is the result
 524 of an imbalance of cellular energy allocation (called the metabolic hypothesis) (Ruoff et al, 2007;
 525 Poertner, 2012; Zakhartsev et al, 2015). The use of metabolic models under non-balanced growth
 526 should be used to challenge this problematic (Baroukh, 2014). Additionally, models describing the
 527 dynamics of acclimation should be used to tackle the cellular response to temperature variations
 528 at different time-scales (Ras et al, 2013).

529 This work is a step towards the comprehension of the effect of global warming on phytoplankton.
 530 To do so, new thermal models should be designed to represent the temperature coupling with
 531 the most important growth factors. For phytoplankton, some models accounting for light and
 532 temperature have been validated on experimental data (Bernard and Rémond, 2012), but we do
 533 not know in which extent they can be used. For example, the effect of temperature at high light
 534 intensity has not clearly been investigated. The development of cell-scaled models representing
 535 the different states of the photosystem centers and their temperature sensitivities (as done, for
 536 example, by Duarte (1995)) should help to better understand the temperature and light coupling.

537 For nutrients, the coupling effect of temperature and starvation have a drastic impact on growth,
538 and models are in development (Thomas, 2013; Thomas et al, 2017).

539 It is worth noting that we did not describe adaptation models at the evolutionary time-scale
540 which are needed to understand long time effects of an increase in temperature on the thermal
541 response. These models, mostly based on the adaptive dynamics theory, are currently being de-
542 veloped (Thomas, 2013; Grimaud, 2016) and should be the next stage to understand the effect of
543 global warming on oceans.

Acknowledgements This work was supported by the ANR Purple Sun project ANR-13-BIME-004. We are grateful to Quentin Béchet, Colin Kremer, Mridul Thomas and the Litchman&Klausmeier lab for their interesting comments on the paper.

References

- Akaike H (1992) Information theory and an extension of the maximum likelihood principle. In: Breakthroughs in statistics, Springer, pp 610–624
- Arrhenius S (1889) On the reaction velocity of the inversion of cane sugar by acids. *Zeitschrift für Physikalische Chemie* 4:226–248
- Augustin JC, Carlier V (2000) Modelling the growth rate of *listeria monocytogenes* with a multiplicative type model including interactions between environmental factors. *International Journal of Food Microbiology* 56(1):53–70
- Baranyi J, Roberts TA (1995) Mathematics of predictive food microbiology. *International journal of food microbiology* 26(2):199–218
- Baranyi J, Robinson T, Kaloti A, Mackey B (1995) Predicting growth of *brochothrix thermosphacta* at changing temperature. *International journal of food microbiology* 27(1):61–75
- Baroukh C (2014) Metabolic modeling under non-balanced growth. application to microalgae for biofuels production. PhD thesis, Université Montpellier 2
- Bernard O, Rémond B (2012) Validation of a simple model accounting for light and temperature effect on microalgal growth. *Bioresource Technology* 123:520–527
- Bernard O, Mairet F, Chachuat B (2015) Modelling of microalgae culture systems with applications to control and optimization. In: *Microalgae Biotechnology*, Springer, pp 59–87
- Bischof JC, He X (2005) Thermal stability of proteins. *N Y Acad Sci* 1066:12–33
- Blanchard GF, Guarini JM, Richard P, Gros P, Mornet F (1996) Quantifying the short-term temperature effect on light-saturated photosynthesis of intertidal microphytobenthos. *Marine Ecology Progress Series* 134:309–313
- Boyd PW, Rynearson TA, Armstrong EA, Fu F, Hayashi K, Hu Z, Hutchins DA, Kudela RM, Litchman E, Mulholland MR, Passow U, Strzepek RF, Whittaker KA, Yu E, Thomas MK (2013) Marine phytoplankton temperature versus growth responses from polar to tropical waters outcome of a scientific community-wide study. *PLoS ONE* 8:e63,091, DOI 10.1371/journal.pone.0063091
- Brauer V, Stomp M, Rosso C, van Beusekom S, Emmerich B, Stal L, Huisman J (2013) Low temperature delays timing and enhances the cost of nitrogen fixation in the unicellular cyanobacterium *cyanoshece*. *The ISME journal* 13:1–11
- Campbell A (1957) Synchronization of cell division. *Bacteriological Reviews* 21(4):263
- Caspeta L, Chen Y, Ghiaci P, Feizi A, Buskov S, Hallström BM, Petranovic D, Nielsen J (2014) Altered sterol composition renders yeast thermotolerant. *Science* 346(6205):75–78
- Chen P, Shakhnovich EI (2010) Thermal adaptation of viruses and bacteria. *Biophysical journal* 98(7):1109–1118
- Corkrey R, McMeekin TA, Bowman JP, Ratkowsky DA, Olley J, Ross T (2014) Protein thermodynamics can be predicted directly from biological growth rates. *PloS one* 9(5):e96,100
- Corradini MG, Peleg M (2006) On modeling and simulating transitions between microbial growth and inactivation or vice versa. *International journal of food microbiology* 108(1):22–35
- Danson MJ, Hough DW, Russell RJ, Taylor GL, Pearl L (1996) Enzyme thermostability and thermoactivity. *Protein engineering* 9(8):629–630

- Dermoun D, Chaumont D, Thebault JM, Dauta A (1992) Modelling of growth of porphyridium cruentum in connection with two interdependent factors: light and temperature. *Bioresource technology* 42(2):113–117
- Dill KA, Ghosh K, Schmit JD (2011) Physical limits of cells and proteomes. *Proceedings of the National Academy of Sciences* 108(44):17,876–17,882
- Droop M (1968) Vitamin b12 and marine ecology. iv. the kinetics of uptake, growth and inhibition in *monochrysis lutheri*. *J Mar Biol Assoc UK* 48(3):689–733
- Duarte P (1995) A mechanistic model of the effects of light and temperature on algal primary productivity. *Ecological Modelling* 82(2):151–160
- Edwards KF, Thomas MK, Klausmeier CA, Litchman E (2016) Phytoplankton growth and the interaction of light and temperature: A synthesis at the species and community level. *Limnology and Oceanography*
- Eijsink VG, Gåseidnes S, Borchert TV, van den Burg B (2005) Directed evolution of enzyme stability. *Biomolecular engineering* 22(1):21–30
- Eppley RW (1972) Temperature and phytoplankton growth in the sea. *Fish Bull* 70:1063–1085
- Eyring H (1935) The activated complex in chemical reactions. *The Journal of Chemical Physics* 3(2):107–115
- Falkowski PG, Raven JA (2013) *Aquatic photosynthesis*. Princeton University Press
- Field CB, Behrenfeld MJ, Randerson JT, Falkowski PG (1998) Primary production of the biosphere: integrating terrestrial and oceanic components. *Science* 281:237
- Follows MJ, Dutkiewicz S, Grant S, Chisholm SW (2007) Emergent biogeography of microbial communities in a model ocean. *science* 315(5820):1843–1846
- Frauenfelder H, Sligar SG, Wolynes PG (1991) The energy landscapes and motions of proteins. *Science* 254(5038):1598–1603
- Frey SD, Lee J, Melillo JM, Six J (2013) The temperature response of soil microbial efficiency and its feedback to climate. *Nature Climate Change* 3(4):395–398
- Fuhrman JA, Cram JA, Needham DM (2015) Marine microbial community dynamics and their ecological interpretation. *Nature Reviews Microbiology* 13(3):133–146
- Geider R (1987) Light and temperature dependence of the carbon to chlorophyll a ratio in microalgae and cyanobacteria: implications for physiology and growth of phytoplankton. *New Phytol* 106(1):1–34
- Geider RJ, MacIntyre KL, Kana TM (1998) A dynamic regulatory model of phytoplanktonic acclimation to light, nutrients, and temperature. *Limnology and Oceanography* 43:679–694
- van Gestel NC, Reischke S, Bååth E (2013) Temperature sensitivity of bacterial growth in a hot desert soil with large temperature fluctuations. *Soil Biology and Biochemistry* 65:180–185
- Ghosh K, Dill K (2010) Cellular proteomes have broad distributions of protein stability. *Biophysical journal* 99(12):3996–4002
- Ghosh K, de Graff AM, Sawle L, Dill KA (2016) The role of proteome physical chemistry in cell behavior. *The Journal of Physical Chemistry B*
- Gillooly JF, Brown JH, West GB, Savage VM, Charnov EL (2001) Effects of size and temperature on metabolic rate. *science* 293(5538):2248–2251
- Grimaud GM (2016) Modelling the effect of temperature on phytoplankton growth: from acclimation to adaptation. PhD thesis, Université de Nice-Sophia Antipolis
- Hall EK, Singer GA, Kainz MJ, Lennon JT (2010) Evidence for a temperature acclimation mechanism in bacteria: an empirical test of a membrane-mediated trade-off. *Functional Ecology* 24(4):898–908
- Hinshelwood CN (1945) *The chemical kinetics of bacterial cells*. Oxford at the Clarendon press
- Hobbs JK, Jiao W, Easter AD, Parker EJ, Schipper LA, Arcus LV (2013) Change in heat capacity for enzyme catalysis determines temperature dependence of enzyme catalyzed rates. *ACS Chemical Biology* 8:2388–2393
- Holcomb DL, Smith MA, Ware GO, Hung YC, Brackett RE, Doyle MP (1999) Comparison of six dose-response models for use with food-borne pathogens. *Risk Analysis* 19(6):1091–1100
- Jensen S, Knutsen G (1993) Influence of light and temperature on photoinhibition of photosynthesis in *spirulina platensis*. *Journal of applied phycology* 5(5):495–504
- Johnson FH, Lewin I (1946) The growth rate of *e. coli* in relation to temperature, quinine and coenzyme. *Journal of Cellular and Comparative Physiology* 28(1):47–75

- Kingsolver JG (2009) The well-temperated biologist. *The American Naturalist* 174:755–768
- Kooijman SALM (2010) Dynamic energy budget theory for metabolic organisation. Cambridge university press
- Leuenberger P, Gansch S, Kahraman A, Cappelletti V, Boersema PJ, von Mering C, Claassen M, Picotti P (2017) Cell-wide analysis of protein thermal unfolding reveals determinants of thermostability. *Science* 355(6327):eaai7825
- Li Z, Srivastava P (2004) Heat-shock proteins. *Current Protocols in Immunology* pp A–1T
- Lloyd J, Taylor J (1994) On the temperature dependence of soil respiration. *Functional ecology* pp 315–323
- Lobry JR, Rosso L, Flandrois JP (1991) A fortran subroutine for the determination of parameter confidence limits in non-linear models. *Binary* 3:86–93
- Mafart P, Couvert O, Gaillard S, Leguérinel I (2002) On calculating sterility in thermal preservation methods: application of the weibull frequency distribution model. *International journal of food microbiology* 72(1):107–113
- Moats WA (1971) Kinetics of thermal death of bacteria. *Journal of Bacteriology* 105(1):165–171
- Murphy KP, Gill SJ (1991) Solid model compounds and the thermodynamics of protein unfolding. *Journal of molecular biology* 222(3):699–709
- Murphy KP, Privalov PL, Gill SJ (1990) Common features of protein unfolding and dissolution of hydrophobic compounds. *Science* 247(4942):559–561
- Norberg J (2004) Biodiversity and ecosystem functioning: A complex adaptive systems approach. *Limnol Oceanogr* 49:1269–1277
- Paul EA (2014) Soil microbiology, ecology and biochemistry. Academic press
- Peeters J, Eilers P (1978) The relationship between light intensity and photosynthesis a simple mathematical model. *Hydrobiological Bulletin* 12(2):134–136
- Pena MI, Davlieva M, Bennett MR, Olson JS, Shamoo Y (2010) Evolutionary fates within a microbial population highlight an essential role for protein folding during natural selection. *Molecular systems biology* 6(1)
- Pittera J, Humily F, Thorel M, Grulois D, Garczarek L, Six C (2014) Connecting thermal physiology and latitudinal niche partitioning in marine synechococcus. *The ISME Journal* 118:1751–7370
- Poertner HO (2012) Integrating climate-related stressor effects on marine organisms: unifying principles linking molecule to ecosystem-level changes. *Marine Ecology Progress Series* 470:273–290
- Pomeroy LR, Wiebe WJ (2001) Temperature and substrates as interactive limiting factors for marine heterotrophic bacteria. *Aquatic Microbial Ecology* 23(2):187–204
- Privalov P, Khechinashvili N (1974) A thermodynamic approach to the problem of stabilization of globular protein structure: a calorimetric study. *Journal of molecular biology* 86(3):665–684
- Privalov PL (1979) Stability of proteins small globular proteins. *Advances in protein chemistry* 33:167–241
- Ras M, Steyer JP, Bernard O (2013) Temperature effect on microalgae: a crucial factor for outdoor production. *Reviews in Environmental Science and Bio/Technology* 12(2):153–164
- Ratkowsky D, Lowry R, McMeekin T, Stokes A, Chandler R (1983) Model for bacterial culture growth rate throughout the entire biokinetic temperature range. *Journal of Bacteriology* 154:1222–1226
- Ratkowsky D, Olley J, McMeekin TA, Ball A (1982) Relationship between temperature and growth rate of bacterial cultures. *Journal of Bacteriology* 149(1):1–5
- Ratkowsky DA, Olley J, Ross T (2005) Unifying temperature effects on the growth rate of bacteria and the stability of globular proteins. *Journal of theoretical biology* 233(3):351–362
- Robertson AD, Murphy KP (1997) Protein structure and the energetics of protein stability. *Chemical reviews* 97(5):1251–1268
- Rogelj J, Meinshausen M, Knutti R (2012) Global warming under old and new scenarios using ipcc climate sensitivity range estimates. *Nature climate change* 2(4):248–253
- Rosenberg B, Kemeny G, Switzer RC, Hamilton TC (1971) Quantitative evidence for protein denaturation as the cause of thermal death. *Nature* (232):471–473
- Ross T (1993) A philosophy for the development of kinetic models in predictive microbiology. PhD thesis, University of Tasmania
- Rosso L, Lobry J, Flandrois J (1993) An unexpected correlation between cardinal temperatures of microbial growth highlighted by a new model. *J Theor Biol* 162:447–463

- Ruoff P, Zakhartsev M, Westerhoff HV (2007) Temperature compensation through systems biology. *FEBS journal* 274(4):940–950
- Sawle L, Ghosh K (2011) How do thermophilic proteins and proteomes withstand high temperature? *Biophysical journal* 101(1):217–227
- Schipper LA, Hobbs JK, Ruledge S, Arcus VL (2014) Thermodynamic theory explains the temperature optima of soil microbial processes and high q_{10} values at low temperatures. *Global Change Biology* 20:3578–3586
- Schwarz G, et al (1978) Estimating the dimension of a model. *The annals of statistics* 6(2):461–464
- Serra-Maia R, Bernard O, Gonçalves A, Bensalem S, Lopes F (2016) Influence of temperature on *Chlorella vulgaris* growth and mortality rates in a photobioreactor. *Algal Research* 18:352–359
- Slator A (1916) Ii.the rate of growth of bacteria. *Journal of the Chemical Society, Transactions* 109:2–10
- Smelt J, Brul S (2014) Thermal inactivation of microorganisms. *Critical reviews in food science and nutrition* 54(10):1371–1385
- Smelt JP, Hellemons JC, Wouters PC, van Gerwen SJ (2002) Physiological and mathematical aspects in setting criteria for decontamination of foods by physical means. *International Journal of Food Microbiology* 78(1):57–77
- Snyder CD (1906) The influence of temperature upon the rate of heart beat in the light of the law for chemical reaction velocity.ii. *American Journal of Physiology–Legacy Content* 17(4):350–361
- Song Y, Chen Q, Ci D, Shao X, Zhang D (2014) Effects of high temperature on photosynthesis and related gene expression in poplar. *BMC plant biology* 14(1):111
- Taucher J, Jones J, James A, Brzezinski M, Carlson C, Riebesell U, Passow U (2015) Combined effects of CO₂ and temperature on carbon uptake and partitioning by the marine diatoms *Thalassiosira weissflogii* and *Dactyliosolen fragilissimus*. *Limnology and Oceanography*
- Thomas M (2013) The effect of temperature on the ecology, evolution, and biogeography of phytoplankton. PhD thesis, Michigan State University
- Thomas M, Kremer C, Klausmeier C, Litchman E (2012) A global pattern of thermal adaptation in marine phytoplankton. *Science* 338:1085–1088
- Thomas MK, Litchman E (2016) Effects of temperature and nitrogen availability on the growth of invasive and native cyanobacteria. *Hydrobiologia* 763(1):357–369
- Thomas MK, Aranguren-Gassis M, Kremer CT, Gould MR, Anderson K, Klausmeier CA, Litchman E (2017) Temperature-nutrient interactions exacerbate sensitivity to warming in phytoplankton. *Global Change Biology*
- Valik L, Medvedova A, Cizniar M, Liptakova D (2013) Evaluation of temperature effect on growth rate of *Lactobacillus rhamnosus* GG in milk using secondary models. *Chemical Papers* 67(7):737–742
- Van Uden N (1985) Temperature profiles of yeasts. *Advances in microbial physiology* 25:195–251
- Vezzulli L, Brettar I, Pezzati E, Reid PC, Colwell RR, Höfle MG, Pruzzo C (2012) Long-term effects of ocean warming on the prokaryotic community: evidence from the vibrios. *The ISME journal* 6(1):21–30
- Young JN, Goldman JA, Kranz SA, Tortell PD, Morel FM (2015) Slow carboxylation of rubisco constrains the rate of carbon fixation during antarctic phytoplankton blooms. *New Phytologist* 205(1):172–181
- Zakhartsev M, Yang X, Reuss M, Pörtner HO (2015) Metabolic efficiency in yeast *Saccharomyces cerevisiae* in relation to temperature dependent growth and biomass yield. *Journal of thermal biology* 52:117–129
- Zeldovich KB, Chen P, Shakhnovich EI (2007) Protein stability imposes limits on organism complexity and speed of molecular evolution. *Proceedings of the National Academy of Sciences* 104(41):16,152–16,157
- Zhang J (2000) Protein-length distributions for the three domains of life. *Genome Analysis* 16(3):107–109
- Zwietering MH, Wiltjes T, Rombouts FM, van't Riet K (1993) A decision support system for prediction of microbial spoilage in foods. *Journal of Industrial Microbiology* 12(3-5):324–329